Available online at www.sciencedirect.com

SciVerse ScienceDirect

Ceramics International 39 (2013) 7015–7021

CERAMICS INTERNATIONAL

www.elsevier.com/locate/ceramint

Relationship between printability and rheological behavior of ink-jet conductive inks

Kyoohee Woo, Daehwan Jang, Youngwoo Kim, Jooho Moon*

Department of Materials Science and Engineering, Yonsei University, 50 Yonsei-ro Seodaemun-gu, Seoul 120-749, Republic of Korea

Received 11 February 2013; received in revised form 13 February 2013; accepted 14 February 2013
Available online 20 February 2013

Abstract

The application of ink-jet printing technologies suitable for the direct writing of complex patterns requires ink-jet printable inks with appropriate properties. Good ink-jet printability and particle-dispersion stability of inks are necessary for ink-jet printing in a particle-included dispersion system. This study investigates the effects of the rheological properties of silver nanoparticle conductive inks with different dispersion states on printability and ink stability. In addition, the electrical properties (i.e., resistivity) of films that were annealed at temperatures ranging from 300 °C to 500 °C and fabricated by three inks with different dispersion states were measured, revealing that film conductivity was strongly related to the dispersion state of the ink.

Keywords: Ink-jet printing; Silver conductive ink; Rheology; Dispersion; Printability

1. Introduction

Ink-jet printing is one of the most promising technologies and is suitable to produce complex patterns through low-cost direct writing of functional inks on various substrates [1–7]. Recently, ink-jet printing has been adopted to fabricate polymeric electroluminescent devices, controlled-release drug delivery devices, radio-frequency identification tags, and refractive micro-lenses made of hybrid organic–inorganic materials [2,8,9]. The drop-on-demand (DOD) mode is most commonly used in ink-jet printing for modern industrial applications. This method deposits a precise quantity of functional ink in the form of droplets on an arbitrary surface by applying a short pressure pulse through a nozzle which is typically 20–50 μm in diameter [10]. The jetting operation mechanism involves the generation of pressure waves in an ink-filled pathway behind an orifice. At the end of the orifice, the ink meniscus is maintained by surface tension. A piezoelectrically-induced pressure wave can propagate against the surface tension of the ink, forming a small droplet that is then ejected from the nozzle.

By continuing refinement and advancement in multi-layering and fine-line patterning of microelectronics, the use of proper ink formulations has become of practical importance in meeting emerging requirements for further miniaturization of microelectronics and for higher reliability performance. Inappropriate dispersion state of the ink will lead to unstable ink-jetting, resulting in a deflected ejection and longer filament formation [11]. In other words, the dispersion state of the ink influences the positional accuracy and the resolution of the printing as well as the printability of the ink. Therefore, the formulation of functional inks has to be carefully controlled for high precision ink-jet printing.

The critical parameters of printing inks are viscosity, density, and surface tension. These fluid properties influence the mechanism of drop formation and subsequent drop size at a given voltage. Ink formulators often encounter problems where slight alterations in ink composition may cause inconsistencies in ink-jet performances and printing quality, even though the formulation and physical properties are fairly similar. Predicting the reliability of the ink in terms of its basic physical properties

*Corresponding author. Tel.: +82 2 2123 2855; fax: +82 2 312 5375.
E-mail address: jmoon@yonsei.ac.kr (J. Moon).

0272-8842/$ - see front matter © 2013 Elsevier Ltd and Techna Group S.r.l. All rights reserved.
http://dx.doi.org/10.1016/j.ceramint.2013.02.039

such as viscosity and surface tension is difficult because there are many intrinsic physical and chemical properties that contribute to the overall printability of inks [12]. In this study, the influence of the dispersion state was investigated in terms of printability, printing accuracy, and resulting film properties. Printing characteristics were observed by the *in situ* monitoring of droplet formation dynamics using the conductive inks of different stability states, i.e., *normal*, *stable*, and *unstable* dispersions. Moreover, the conductivity and microstructure of the printed Ag films from the conductive inks were examined as a function of the annealing temperature.

2. Experimental procedure

The conductive ink was prepared using commercially available Ag nanoparticles (Changsung Corporation, Korea). The average diameter and specific surface area of the Ag nanoparticles were 74 nm and 8.9 $m^2 g^{-1}$, respectively. The Ag nanoparticles were dispersed in a mixed solvent of ethylene glycol (EG, 99.9%, Aldrich, UK) and deionized water. The dispersion was stirred vigorously at 250 rpm for 1 h in a planetary mill (PM100, Retsch, Germany), followed by filtration through a 5 μm nylon mesh. The solid loading of the conductive inks was 10 wt%. The dispersant, Hypermer KD-3 (ICI Chemicals, London, UK), was used to modify the dispersion state of the inks. KD-3 is a polyimine ester copolymer consisting of carboxylic acid, imine functional groups and polyester stabilizing moieties. The flow and oscillation of the prepared silver inks were measured by a Peltier concentric-cylinder double-gap rheometer (AR2000ex, TA Instruments Inc., UK).

To investigate drop formation and positioning error, an ink-jet printing system consisting of a nozzle, a jetting driver (pressure pulse generating system), a charge-coupled device (CCD) camera, and a system computer was utilized. The ink-jet nozzle with an orifice diameter of 50 μm was manufactured by MicroFab Technologies, Inc. (Plano, TX). This employed a radial polarized lead zirconate titanate (PZT) type 5H tube actuator, with electrodes on the inner and outer cylindrical faces. The nozzle was rigidly bonded to a glass tube with epoxy. The print head was mounted on a computer-controlled three-axis gantry system capable of movements accurate to ± 5 μm. In ink-jet printing, it is important to operate at conditions of pressure suitable for stable drop formation. To address this, a well-conditioned pressure wave form was kept constant. A bipolar waveform that consisted of a succession of two square-wave (positive and negative) pulses was used and allowed for a high voltage difference without the need for excessive high pulse amplitude. The dwell time was set at 3 μs, and the echo time was set to be three times longer. The dwell and echo voltages were set at $+20$ and -20 V, respectively. The gap between the nozzle and the surface was kept at 0.5 mm during printing. The CCD camera took snapshots of the drop formation dynamics with an inter-frame time of 1 μs. The camera was equipped with a strobe LED light to view individual droplets and measure their sizes and travel velocities. The drop dynamics were captured by increasing the delay time of the camera in steps of 1 μs. Droplet images were taken at various delay intervals, showing the flight distance from the nozzle tip. The printing was carried out at a relative humidity of 40% at 25 °C. The printed silver films were annealed in air on a hot plate at predetermined temperatures ranging from 300 to 500 °C for 30 min at a constant heating rate of 5 °C min^{-1}. The surface microstructure of the films was observed by scanning electron microscopy (SEM, JSM-6700F, JEOL), and the film resistivity was calculated from the sheet resistance and film thickness measured by a 4-point probe (CMT-SR200N, Chang Min Co., Ltd.) and surface profiler (Dektak 150, Veeco), respectively.

3. Results and discussion

Adsorption of surfactant and polymer molecules on the surface of the particles may affect stability and rheological behavior of the dispersion [13–16]. When forced to shear, the dispersions show different responses to deformation rate depending upon general physical and chemical characteristics of the system. Fig. 1a presents plots of viscosity as a function of shear rate for the 10 wt% silver inks containing different dispersant (Hypermer KD-3) amounts. All inks exhibited distinctive pseudoplastic (shear-thinning flow) behavior, which is characterized by a decrease in the viscosity with increasing shear rate within a range of 0–100 s^{-1}. The attraction between the silver particles induces flocculation in the inks, which causes an immobility of the solvent suspending the particles and in turn increases the viscosity at low shear rate [17]. In contrast, under the influence of a higher shear rate, the flocculation breaks down and promotes the mobility of solvent entrapped between particles, lowering the viscosity. The viscosity of the inks decreased upon the addition of dispersant, achieving a minimum value at approximately 2 wt%. In this case, the polymeric dispersant molecules absorbed on the particle surfaces acted as an effective layer for steric stabilization to prevent the particles from agglomerating in the solvent, resulting in a decrease of the viscosity. However, the viscosity increased when more than 2 wt% of the dispersant was added. It is believed that, in the case of ink with greater than 2 wt% of dispersant, the excess dispersant was not adsorbed on the surface of the particles, and the non-adsorbing free polymers in the suspension deteriorated the suspension stability and increased the viscosity. For further information regarding ink stability, the relative viscosity of the inks was analyzed at very high shear rates similar to the range experienced during ink-jet printing (usually on the order of 10^5 s^{-1}), as shown in Fig. 1b. The relative viscosity, defined as the viscosity of the suspension divided by that of the medium, can be used as a measure of the degree of flocculation [18,19]. The relative viscosity decreased until its

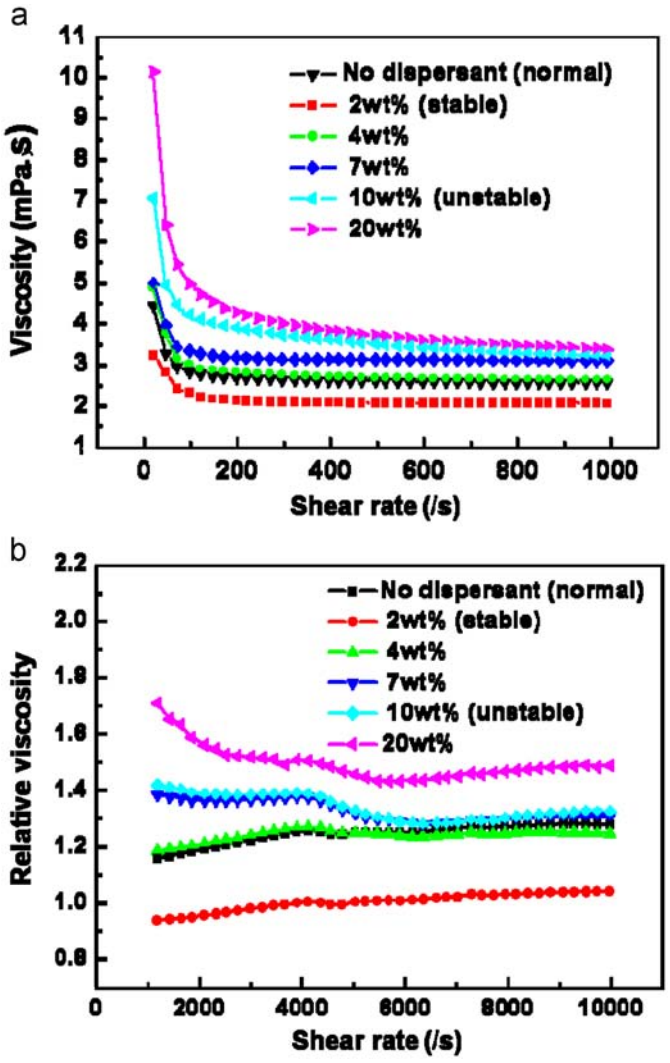

Fig. 1. Plots of viscosity variation as a function of shear rate: (a) shear rate 1–1000 s^{-1} and (b) shear rate 1000–10000 s^{-1}.

minimum at 2 wt% dispersant and then increased with the addition of more dispersant. The trend of relative viscosity according to the amount of dispersant was similar, with the result shown in Fig. 1a, implying that the amount of dispersant plays an important role in dispersion stability, and the addition of a proper amount of dispersant is necessary to prepare well-dispersed, conductive inks with a low viscosity (~2 mPa s at 50 s^{-1}).

Fig. 2 shows the yield stress variation as a function of dispersant content. The silver inks begin to flow only after the applied stress exceeds a certain critical value, known as yield stress [20,21]. The yield stresses for the inks with varying dispersant contents are obtained based on a simple Bingham model expressed by [22,23]:

$$\tau = \tau_o + \eta\gamma \quad (1)$$

where η is the viscosity, τ is the shear stress for a given shear rate (γ), and τ_o is the yield stress for a zero shear rate. When the 2 wt% dispersant was added, the yield stress reached a minimum value. In the range of 2–7 wt%

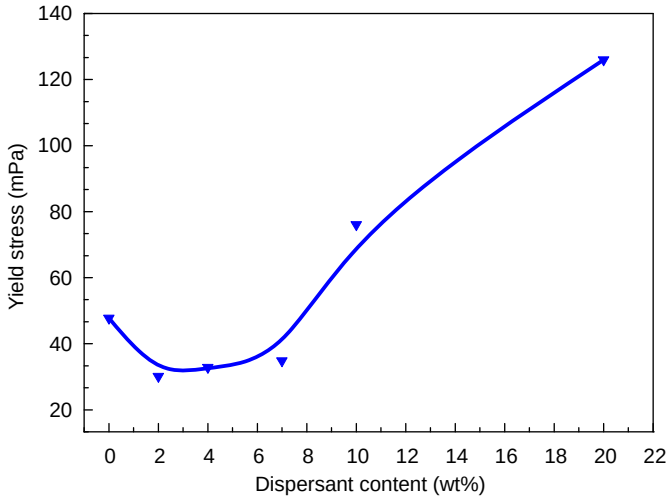

Fig. 2. Yield stress behavior as a function of dispersant content in silver ink.

addition, the yield stress was nearly constant. Above 7 wt%, the increased yield stress was attributed to the presence of excess polymers in solution. These findings are in good agreement with the result of viscosity measurement in which the optimal dispersant concentration was determined to be 2 wt%.

To investigate the inter-relationship between rheological properties and ink printability, three inks were tested with different dispersion states categorized as *stable*, *unstable*, and *normal* dispersions. *Stable* and *unstable* dispersions were the 2 and 10 wt% dispersant added Ag inks, respectively, whereas the *normal* dispersion was ink without the dispersant. The response of the complex inks to small amplitude oscillatory shear flows was investigated to understand the influence of the added dispersant on the suspension stability. Fig. 3 shows a log–log plot of the elastic (G') and viscous (G'') moduli as a function of frequency range of 0.1–500 rad s^{-1} for each ink with a characteristic dispersion state. G' and G'' can be thought of as a measure of stiffness and viscous resistance to deformation, respectively [24]. For the *normal* dispersion (Fig. 3a), G' was higher than G'' at low frequency, indicative of a predominant elastic response. This could be due to significant compression and interpenetration of the stabilizing polymer molecules. However, at high frequency, G'' was higher than G', implying a predominant viscous response. This observation would be related to the influence of hydrodynamic forces, as the particles do not experience a strong attractive force since the stabilizing dispersant molecules do not overlap at high frequency. As such, *normal* dispersion exhibited both elastic and viscous responses depending upon the shearing frequency. In the case of the *stable* dispersion, G'' was always higher than G'. This reflected a relatively weak attraction between Ag particles from which the particles were well separated from each other in the ink regardless of frequency. On the contrary, in the case of the *unstable* dispersion, G' was generally higher than G'', and this indicated strong

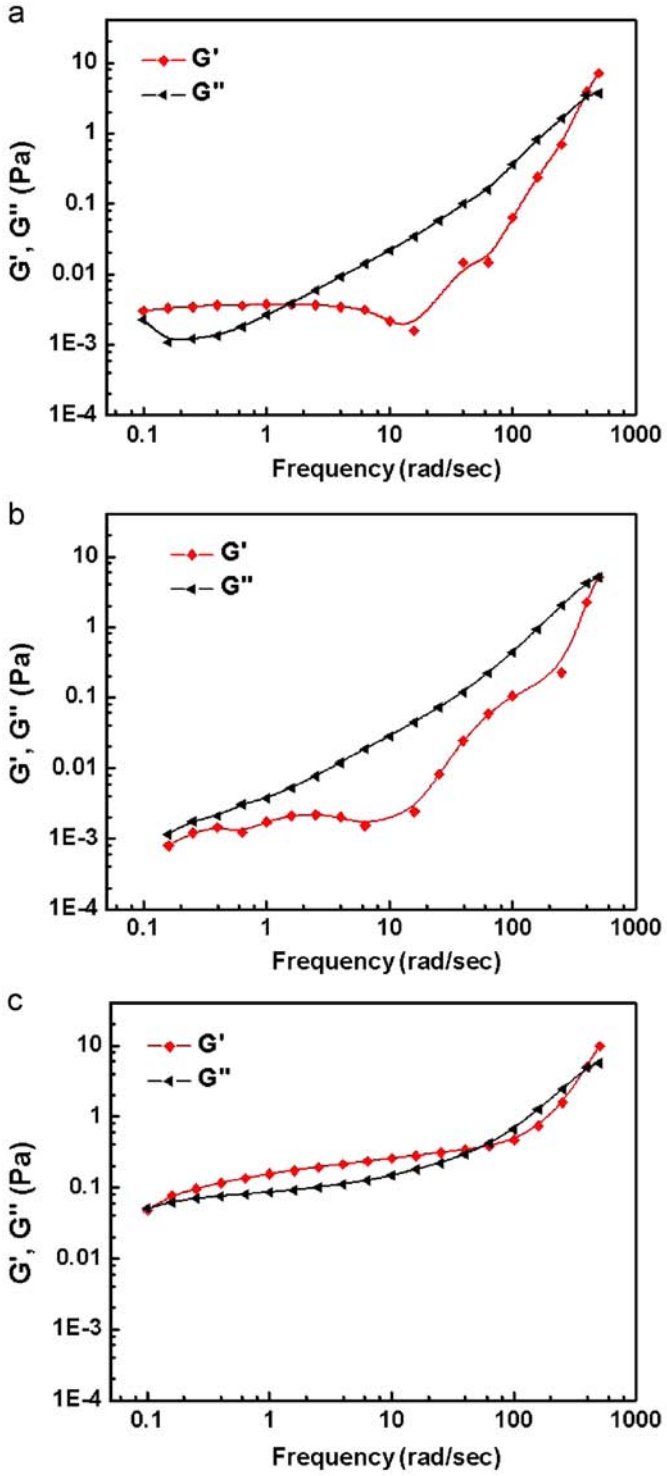

Fig. 3. A log–log plot of the elastic (G') and viscous (G'') moduli as a function of frequency range from 0.1 to 500 rad sec^{-1}: (a) *normal* dispersion, (b) *stable* dispersion, and (c) *unstable* dispersion.

interparticle attraction such that the ink behaved as a partially flocculated fluid [25].

Using three inks with different dispersion states, droplet formation dynamics were observed which were manifested by the ink's response to an applied pressure stimulus during piezoelectric DOD ink-jet printing. Drop ejection is the result of the superposition of consecutive acoustic waves that generate pressure pulses large enough to overcome the viscous dissipation and the energy associated with the formation of a new surface [26,27]. Fig. 4 shows a representative photo sequence of drop formation for fluids with different contents of dispersant at a constant driving voltage of 20 V. The dynamics of droplet formation as a function of dispersant content were different depending upon the state of dispersion. The pressure pulse pushed the fluid out of the nozzle tip, and the meniscus bulged quickly until a filament with a round head formed at an elapsed time of 20–30 μs. The traveling velocity difference between the droplet head and end stretched the droplet filament until an elapsed time of about 50–60 μs. During the stretching of the fluid filament, the tail of the filament near the nozzle tip was continuously necking, forming a long fluid filament. The recoiling filament nearly detached from the falling droplet, generating a primary droplet and a transient satellite, both of which merged together into a single droplet at an elapsed time of 70–80 μs for the *normal* dispersion (Fig. 4a) and 60–70 μs for the *stable* (Fig. 4b) dispersions. For the *unstable* dispersion (Fig. 4c), however, the single droplet formation occurred at a prolonged time (100 μs), and blurred images of the droplets indicate that the trajectory of the droplets ejected from the *unstable* dispersion was angled.

From the images in Fig. 4, the filament length variation as a function of delay time for the inks with varying dispersant content was measured and plotted in Fig. 5. For *normal* dispersion, a round protruding head formed on the filament at an elapsed time of about 30 μs, and the filament stretched until a time of about 60 μs. Filament rupture occurred at about 110 μs. In contrast, the *stable* dispersion was subjected to faster filament elongation and earlier rupture. The fluid bulged to form a round filament head at a time of about 30 μs, and filament elongation occurred until about 45 μs. The bulge eventually ruptured at about 90 μs. This observation indicated that a stable droplet can be rapidly formed in the case of the *stable* ink.

To investigate the correlation between the dispersion stability and ink-jet printability, the placement accuracy of droplets (an array of 10×10) jetted from the inks of different dispersion states under a constant applied driving voltage of 20 V and a jetting frequency of 1 kHz was compared at the same x–y moving tables and stand-off distance, as shown in Fig. 6. The landing position of each dot was evaluated with respect to the predetermined target position. The positioning accuracy assessed in this method primarily reflected the flight bending error and the travel velocity variation depending on the state of the dispersion. The positioning error became larger as the state of the dispersion deteriorated. The average radial deviations were 5.5 μm for the *stable* dispersion, 13.8 μm for the *normal* dispersion, and 21.6 μm for the *unstable* dispersion. This observation indicated that rapid and *stable* droplet formation from the *stable* ink could lead to the achievement of

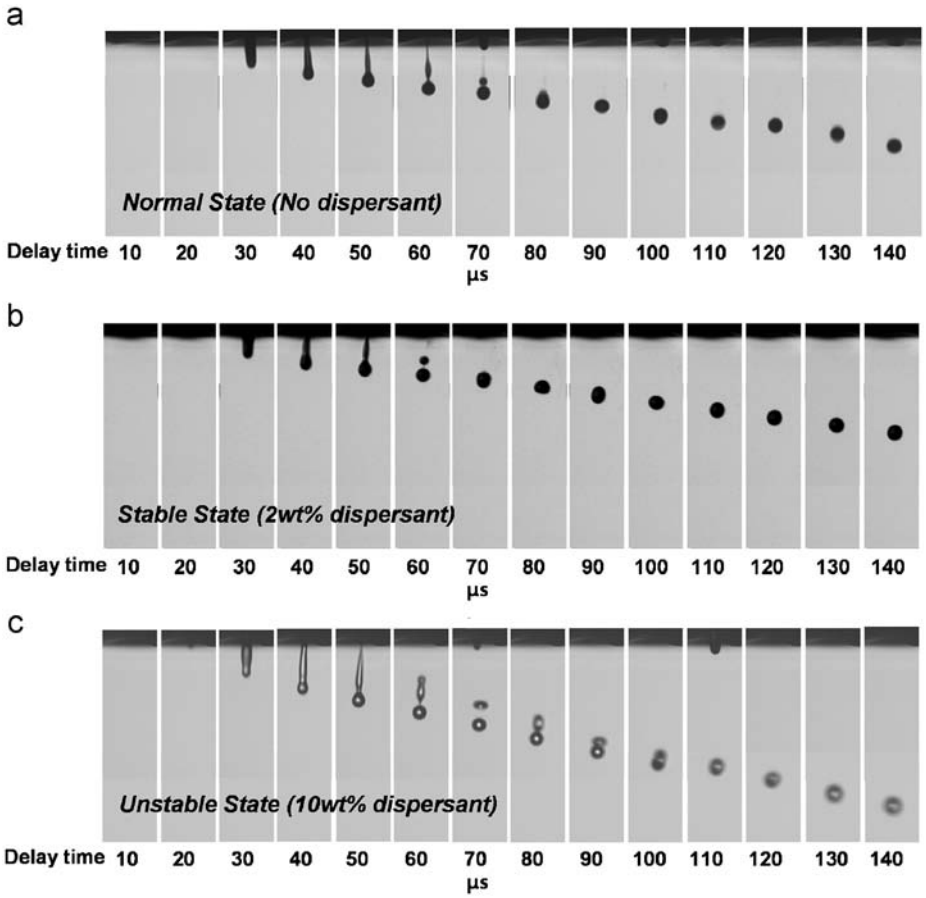

Fig. 4. Representative photo sequence of drop formation for three different silver inks with various dispersant contents at a constant driving voltage of 20 V: (a) *normal* dispersion, (b) *stable* dispersion, and (c) *unstable* dispersion.

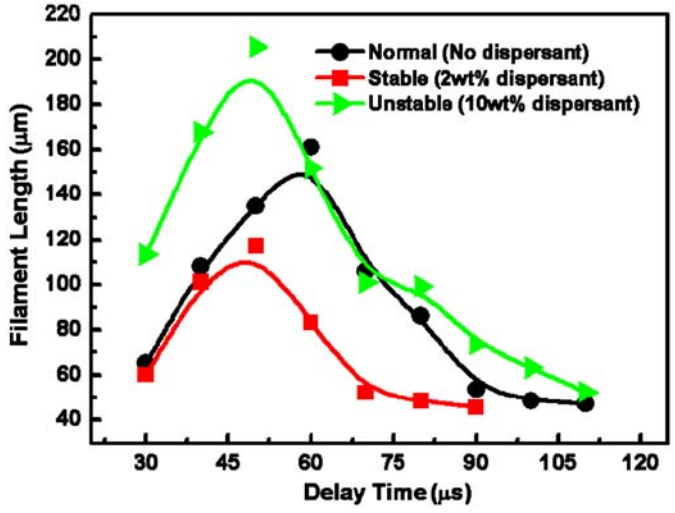

Fig. 5. Filament length variation as a function of delay time for three different silver inks with various dispersant contents.

accurate and high-speed ink-jet printing with better resolution.

On the other hand, the dispersion stability of inks containing particles also had a significant effect on the function of ink. Therefore, the printed films were prepared by ink-jet printing the inks with different dispersion states, and the resistivity variation as a function of the annealing temperatures was investigated, as shown in Fig. 7a. The resistivity of the films obtained from the *stable* dispersion was lower than those fabricated by the *unstable* and *normal* dispersions regardless of the annealing temperature. The resistivity variation was strongly related to particle-dispersing stability. The resistivity difference became clear by observing the films' microstructures annealed at 400 °C, as shown in Fig. 7b. The film printed from the silver ink with *stable* dispersion state had a uniform microstructure with fewer pores, and it exhibited low electrical resistivity due to increased interparticle junctions. On the contrary, films fabricated with *unstable* and *normal* dispersion silver inks had an irregular surface with large pores, revealing relatively higher resistivity than those fabricated with the *stable* ink. The metal nanoparticle compact structure in the as-printed pattern from the *stable* ink had a higher packing density than those from the *normal* and *unstable* inks because the well-dispersed particles were arranged into a densely packed structure during the ink drying. More densely packed Ag particles are easily converted to conductive granular metal films by forming interparticle necking during post-printing thermal annealing.

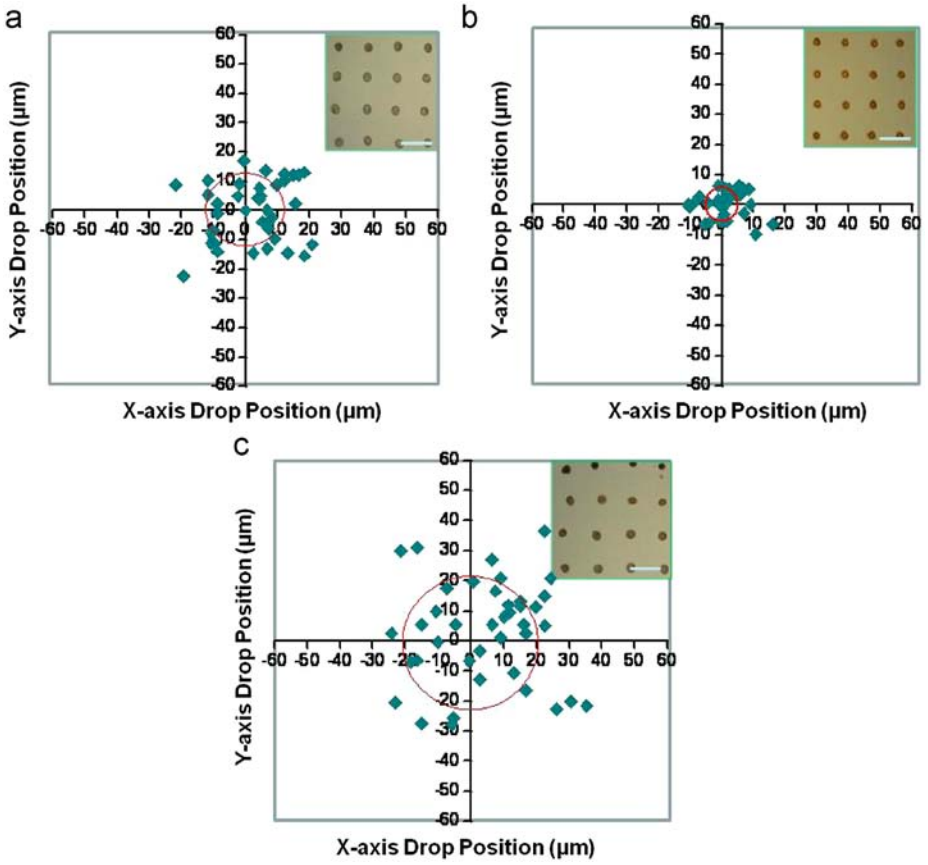

Fig. 6. Drop placement error for the ink-jet printing of three silver inks: (a) *normal* dispersion, (b) *stable* dispersion, and (c) *unstable* dispersion. All scale bars in the insets are 320 μm.

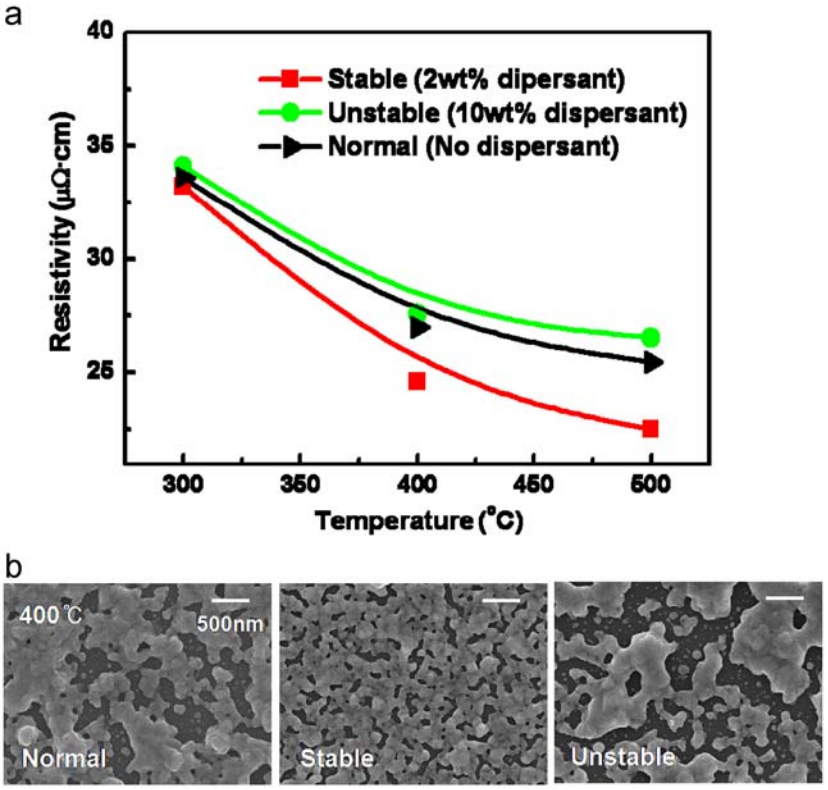

Fig. 7. (a) Resistivity variation as a function of annealing temperature for the films fabricated by three different silver inks with various dispersant contents and (b) SEM images showing the microstructure of the films (annealed at 400 °C) fabricated by three different silver inks.

4. Conclusions

The relationship between ink-jet printability and rheological properties was investigated. A polymeric surfactant consisting of an oligomer polyester reduced the flow resistance of silver particles. The maximum viscosity reduction by the addition of 2 wt% dispersant was found at low and high shear rate regimes (1–1000 and 1000–10000 s^{-1}). The polymeric molecules absorbed on the particle surfaces were thought to provide an effective layer for steric stabilization, which kept the particles suspended and from agglomerating. The dispersion state of the inks was modified by adding differing amounts of the dispersant (no dispersant added, 2 wt% dispersant added, and 10 wt% dispersant added). This allowed an investigation of the relationship between the dispersion state and the printability by *in situ* monitoring jetting dynamics with an image system with an inter-frame time of 1 μs. The droplet formation behavior was characterized in terms of dispersion states, which are related to the rheological properties of inks. The printability of inks was identified by observing the characteristics of printing such as single droplet formability and positional accuracy. Moreover, by examining the conductivity and microstructure of the printed films, the dispersion state was found to affect the electrical properties of the conductive prints from the functional inks. In this regard, these findings suggest that the formulation of functional inks ought to be carefully controlled in consideration of the rheological behavior and the dispersion state of the ink.

Acknowledgments

This work was supported by a National Research Foundation of Korea (NRF) grant funded by the Korean Government (MEST) (nos. 2012R1A3A2026417 and 2011-8-2048). It was also partially supported by the Second Stage of the Brain Korea 21 Project.

References

[1] B. Derby, N. Reis, Inkjet printing of highly loaded particulate suspensions, MRS Bulletin 28 (2003) 815–818.
[2] B.-J. de Gans, P.C. Duineveld, U.S. Schubert, Inkjet printing of polymers: State of the art and future developments, Advanced Materials 16 (2004) 203–213.
[3] S. Jeong, K. Woo, D. Kim, S. Lim, J. Kim, H. Shin, Y. Xia, J. Moon, Controlling the thickness of the surface oxide layer on Cu nanoparticles for the fabrication of conductive structures by ink-jet printing, Advanced Functional Materials 18 (2008) 679–686.
[4] S. Jeong, D. Kim, J. Moon, Ink-jet-printed organic–inorganic hybrid dielectrics for organic thin-film transistors, Journal of Physical Chemistry C 112 (2008) 5245–5249.
[5] D. Kim, S. Jeong, B. Park, J. Moon, Direct writing of silver conductive patterns: Improvement of film morphology and conductance by controlling solvent compositions, Applied Physics Letters 89 (2006) 264101.
[6] P. Calvert, Inkjet printing for materials and devices, Chemistry of Materials 13 (2001) 3299–3305.
[7] P. Liu, Y. Wu, Y. Li, B.S. Ong, S. Zhu, Enabling gate dielectric design for all solution-processed, high-performance, flexible organic thin-film transistors, Journal of the American Chemical Society 128 (2006) 4554–4555.
[8] T. Xu, J. Jin, C. Gregory, J.J. Hickman, T. Boland, Inkjet printing of viable mammalian cells, Biomaterials 26 (2005) 93–99.
[9] E. Tekin, P.J. Smith, S. Hoeppener, A.M.J. van den Berg, A.S. Susha, A.L. Rogach, J. Feldmann, U.S. Schubert, Inkjet printing of luminescent CdTe nanocrystal–polymer composites, Advanced Functional Materials 17 (2007) 23–28.
[10] H.P. Le, Progress and trends in ink-jet printing technology, Journal of Imaging Science Technology 42 (1998) 49–62.
[11] B.-J. de Gans, E. Kazancioglu, W. Meyer, U.S. Schubert, Ink-jet printing polymers and polymer libraries using micropipettes, Macromolecular Rapid Communications 25 (2004) 292–296.
[12] M.H. Tsai, W.S. Hwang, H.H. Chou, P.H. Hsieh, Effects of pulse voltage on inkjet printing of a silver nanopowder suspension, Nanotechnology 19 (2008) 335304–335312.
[13] S. Lee, U. Paik, S.-M. Yoon, J.-Y. Choi, Dispersant-ethyl cellulose binder interactions at the Ni particle-dihydroterpineol interface, Journal of the American Ceramic Society 89 (2006) 3050–3055.
[14] W.J. Tseng, C.N. Chen, Dispersion and rheology of nickel nanoparticle inks, Journal of Materials Science 41 (2006) 1213–1219.
[15] P. Carriere, J.F. Feller, D. Dupuis, Y. Grehens, Rheological properties of silica dispersions stabilized by stereoregular poly(methyl methacrylate), Journal Colloid Interface Science 272 (2004) 218–224.
[16] A.A. Zaman, P. Singh, B.M. Moudgil, Impact of self-assembled surfactant structures on rheology of concentrated nanoparticle dispersions, Journal of Colloid Interface Science 251 (2002) 381–387.
[17] D.J. Shaw, Introduction to Colloid and Surface Chemistry, fourth ed., Butterworth-Heinemann, Oxford, 1996, pp. 22, 169, 200, 244.
[18] Y. Otsubo, M. Horigome, Effect of associating polymer on the dispersion stability and rheology of suspensions, Korea–Australia Rheology Journal 15 (2003) 27–33.
[19] D. Jang, D. Kim, B. Lee, S. Kim, M. Kang, D. Min, J. Moon, Nanosized glass frit as an adhesion promoter for ink-jet printed conductive patterns on glass substrates annealed at high temperatures, Advanced Functional Materials 18 (2008) 2862–2868.
[20] L.F. Hakim, D.M. King, Y. Zhou, C.J. Gump, S.M. George, A.W. Weimer, Nanoparticle coating for advanced optical, mechanical and rheological properties, Advanced Functional Materials 17 (2007) 3175–3181.
[21] S. Mani, G.S. Grover, S.G. Bike, Linear viscoelastic behavior of copper phthalocyanine dispersions used in printing inks.
[22] Y. Otsubo, Rheological behavior of suspensions flocculated by weak bridging of polymer coils, Journal of Colloid Interface Science 215 (1999) 99–105.
[23] S.R. Raghavan, S.A. Khan, Shear-thickening response of fumed silica suspensions under steady and oscillatory shear, Journal of Colloid Interface Science 185 (1997) 57–67.
[24] S.B. Kharchenko, J.F. Douglas, J. Obrzut, E.A. Grulke, K.B. Migler, Flow-induced properties of nanotube-filled polymer materials, Nature Materials 3 (2004) 564–568.
[25] P.F. Luckham, M.A. Ukeje, Effect of particle size distribution on the rheology of dispersed systems, Journal of Colloid Interface Science 220 (1999) 347–356.
[26] N. Reis, C. Ainsley, B. Derby, Viscosity and acoustic behavior of ceramic suspensions optimized for phase-change ink-jet printing, Journal of the American Ceramic Society 88 (2005) 802–808.
[27] D. Jang, D. Kim, J. Moon, Influence of fluid physical properties on ink-jet printability, Langmuir 25 (2009) 2629–2635.